



Synthesis, Spectroscopic and Biological Activity Studies of Zinc(II) Complexes of N1, N'4-bis((1E,2E)-2-(hydroxyimino)-1-(4-R)-phenylethylidene)terephthalohydrazide Schiff base

JOTIRAM KRISHNA CHAVAN and RAJU MARUTI PATIL*

Department of Chemistry, Institute of Science, Dr. Homi Bhabha State University,
15, Madam Cama Road, Mumbai-400 032, Maharashtra, India.

*Corresponding author E-mail: jkchavanypsc@gmail.com, rajupatilisc2006@gmail.com

<http://dx.doi.org/10.13005/ojc/400308>

(Received: April 24, 2024; Accepted: May 25, 2024)

ABSTRACT

In this work, we have synthesized various zinc metal complexes with different acylhydrazoneoxime derivatives. The synthesis process involved condensation of para-substituted isonitrosoacetophenones (4-R-INAP) and terephthalohydrazide (TPHD). To produce these complexes, we reacted zinc chloride with various 4-substituted isonitrosoacetophenone terephthalohydrazide ligands (4-R-INAP-TPHD), where R= -H, -CH₃, -OCH₃ and -Cl. We employed different physicochemical and spectroscopic methods like elemental analysis, TG-DTA, UV-Visible, FTIR, and NMR spectroscopy, electrical conductance, and magnetic susceptibility to analyze the Schiff's base and zinc metal complexes. In addition, we tested the antibacterial activities of these compounds against selected bacteria strains.

Keywords: Acylhydrazoneoxime ligands, Metal complexes, Spectral analysis, Biological activities.

INTRODUCTION

Schiff bases have consistently generated lots of interest due to their variety in structure, preparational convenience, and wide applications as useful materials. Metal complexes of Schiff bases have also recently gained a lot of interest in academia due to their exceptional biological properties. Hydrazones and acylhydrazoneoximes are used¹ in analytical chemistry for the detection, quantification, and isolation of molecules containing the carbonyl group. Hydrazones and oximes are two major groups of substances that have numerous uses²⁻⁴ in industry, medicine, and the identification

and measurement of different metal ions. Ligands synthesized via condensation of para-substituted isonitrosoacetophenones have wider⁵⁻⁶ applications. These molecules contain a variety⁷⁻¹⁰ of possible bonding sites, including imine nitrogen, azomethine, and carbonyl oxygen. As a result, hydrazones and oximes have received substantial importance in the research field. The synthesis and characterization of new oximes are of great interest due to their coordination behavior and acts as ligands. A wide spectrum of pharmacological actions, including antitubercular, antihelmintic, anticancer, and antibacterial activity, make oxime ligands important in coordination chemistry¹¹⁻¹⁵.



Schiff bases have consistently generated lots of interest because of their variety in structure, preparational convenience, and wide applications¹⁶ as useful materials. Recently, there has been a lot of interest in metal complexes of Schiff bases due to their exceptional biological activity, which includes antibacterial, antifungal, and anticancer properties^{13,14,17}. The Schiff base complexes have been demonstrated to originate from acylhydrazoneoximes, carrying the donor sets¹ N₂O and NO₂ interesting¹⁸⁻¹⁹ biological processes. Oximes and hydrazones are two significant groups of chemicals because of their extensive uses^{1,20-21} in industry, medicine, and the identification and quantification of different metal ions. Coordination and description of acylhydrazoneoximes ligands as well as their metal complexes structures are of great²² interest.

The two most significant groups of chemicals are oximes and hydrazones because of their numerous uses in industry, medicine, and the identification and measurement of different metals²⁰. The synthesis and characterisation of metal complexes with acylhydrazoneoxime ligands are of great interest. Terephthalohydrazide and para substituted²³ isonitrosoacetophenones were condensed in an acidic or basic medium in a 2:1 ratio to create acyl hydrazoneoximes. Copper(II) and Zinc(II) salts can react with hydrazone oxime and dihydrazone moieties to form mono- or binuclear complexes. The nitrogen atoms in the oxime, imine, and amide serve as the coordination points for these compounds with hydrazone and oxime groups, which often function as monoanionic tridentate ligands. On the other hand, dihydrazone-containing compounds operate as dianionic ligands. Coordination occurs with the azomethine nitrogen atoms in the enol tautomeric form²⁰ and the enolic oxygen atoms, depending on the circumstances of the reaction. Zinc has long been known to be an essential cofactor in biological molecules, serving as a Lewis acid catalyst that can easily adopt four, five, or six coordination or as a structural template in protein folding. Schiff base ligand-supported zinc metal complexes are continuously investigated^{4,24-25} particularly for their catalytic, photophysical, and aggregation properties. Depending on the nature of the Schiff's base the Zn(II) ion can attain various coordination numbers and geometries. Terephthalohydrazide and para-substituted isonitrosoacetophenones

were condensed in an acidic or basic medium in a 1:2 ratio to produce acylhydrazoneoximes. The deprotonated enol-imine or keto-amide states of metals can be coordinated²⁶ by the keto hydrazone moiety. These compounds frequently function as tridentate monoanionic ligands, coordinating via oxime groups, imines, and amide nitrogens. They also have oxime groups and hydrazone. Zinc (II) salts and acylhydrazoneoximes can react to form mono- or binuclear complexes.

The Synthesis, characterization, and antibacterial activity of novel zinc(II) complexes [Zn (4-R-INAP-TPHD) Cl], obtained from the acylhydrazoneoxime ligand, are reported in this study as a continuation of our work on the coordination structures and antimicrobial properties of this coordination complexes.

EXPERIMENTAL

Materials

Acylhydrazoneoxime ligands and complexes are synthesized using the highest purity and analytical grade (AR) reagents. Zinc chloride was used directly from S. D. Fine Chemicals after being obtained without further processing. Solvents were normally dried and distilled before being used.

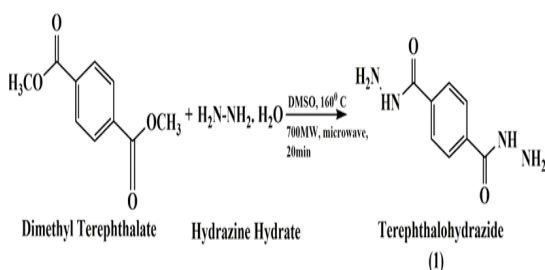
Analytical and Physical measurements

Using KBr pellets, the Shimadzu 8201 PC FT-IR spectrophotometer was used to get the FT-IR spectra (4000-400 cm⁻¹). A Jasco spectrophotometer with a 200–800 nm wavelength range was used to get the absorption spectra (UV–Vis). The ¹H and ¹³C NMR spectral data were obtained via a Bruker AV III HD NMR (500 MHz) in CDCl₃, with Tetra Methyl Silane as a reference. Gouy's Method was utilized to compute the magnetic measurements of metal complexes and dithiocarbamate ligands using magnetic susceptibility balance. In addition, a CHN microanalyzer instrument was used for the percentage of the elements C, H, and N.

Synthesis of Terephthalohydrazide

Dimethyl terephthalate 1.94 g (0.01 mol) was dissolved in 20 cm³ dimethyl sulphoxides (DMSO) as solvent taken in a 100 cm³ flat bottom flask. Then 2 cm³ of Hydrazine hydrate was added to it with constant stirring. This reaction mixture was kept in Raga's open vessel microwave oven system

at 700MW for 20 min with continuous stirring at 160°C temperature. Once the reaction was finished, this flask was kept to cool to room temperature then all the reaction mixture was transferred into a 250 cm³ separating flask and extracted with chloroform to dissolve unreacted dimethyl terephthalate and separated. Then plenty of water was added and shaken well. The separating funnel was kept on standby to allow the settling down of the white precipitate of terephthalohydrazide and then separated by filtration and dried safely. The synthesis of terephthalohydrazide is given in Scheme 1. Yield: 80%; m. p. >300°C, Infrared (KBr, cm⁻¹): 3343 (N-H), 3335 (N-H), 1616 (C=O amide), 1343 (C-N), 736 (Ar-H), 930 (N-N), ¹H-NMR (δ, 400 MHz, DMSO, ppm): 7.87m, 2H (Ar-H), 4.56d, 2H (-NH₂), 9.89t, 1H (-NH), Elemental Analysis: Found (Calculated): C=49.24 (49.48); H=5.04 (5.19); N=28.51 (28.85).



Scheme 1. Synthesis of Terephthalohydrazide (1A)

Preparation of Acylhydrazoneoxime ligands

The substituted acylhydrazoneoxime (INAP-TPHD) ligands were synthesized using a microwave-assisted technique as given in Scheme 2. Refluxing the 2:1 molar of terephthalohydrazide (0.01 mol, 1.94 g), Glacial acetic acid (0.01 mol), 30 cm³ DMSO, and estimated amounts of substituted isonitrosoacetophenone (0.02 mol) in 100 mL flat bottom flask and kept in an open vessel Raga's microwave system at 560 MW for 30 min at 160°C temperature. Then, adding some chloroform to the reaction mixture in a 250 cm³ separation flask and shaken vigorously to dissolve the unreacted reactant and separate. Then, lots of water was added and thoroughly shaken and kept to separate the yellow-coloured acylhydrazoneoxime precipitate to settle down. Then compound was separated and dried.

N¹, N⁴-bis((1E,2E)-2-(hydroxyimino)-1-phenylethylidene)terephthalohydrazide (L1/2A): Yield: 72%, m. p. 190°C, UV-Visible nm(cm⁻¹): 304 (32894.74), 381 (26246.72); Infrared (KBr cm⁻¹): 3413 (O-H), 3140 (N-H), 1644 (CH=N), 1720 (C=O),

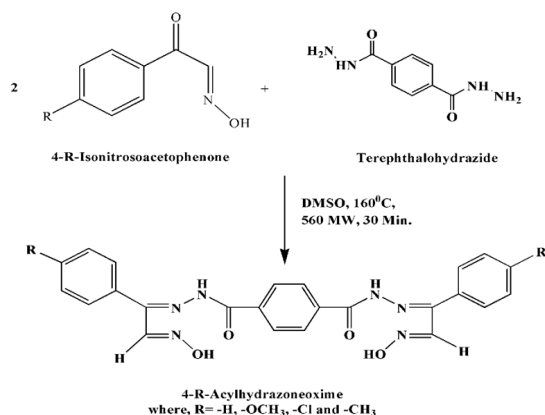
1280 (C-O), 1555 (C=C), 2990 (Csp²-H), 1019 (N-N), 952 (N-O). ¹H-NMR (δ, 400 MHz, DMSO, ppm): 7.36-7.97, multiplet, 14H (Ar-H); 8.29, s, 2H, (-CH=N); 10.59, s, 2H (NH); 12.70, s 2H (OH). ¹³C-NMR (δ, 400 MHz, DMSO, ppm): 127.36, 128.01, 128.68, 129.95, 133.30, 136.57, 145.53, 148.52, 189.51. Mass Spectroscopy Data: 456, 190, 162, 133, 132, 77(Base Peak). Analysis of Elements: Found (Calculated): C=63.04 (63.15); H=4.28 (4.42); N=18.23 (18.41).

N¹, N⁴-bis((1E,2E)-2-(hydroxyimino)-1-(4-methoxyphenyl)ethylidene)terephthalohydrazide (L2/2B): Yield: 70%, m. p. 145°C, UV-Visible nm (cm⁻¹): 299 (33444.82), 376 (26595.74) Infrared (KBr cm⁻¹): 3440 (O-H), 3193 (N-H), 1603 (CH=N), 1685 (C=O), 1167 (C-O), 1576 (C=C), 2982 (Csp²-H), 1028 (N-N), 936 (N-O). ¹H-NMR (δ, 400 MHz, DMSO, ppm): 7.01-7.89, multiplet, 12H (Ar-H); 8.09, s 2H (-CH=N); 10.92, s, 2H (NH); 12.62, s, 2H (OH) & 3.85, s, 6H (-OCH₃). ¹³C-NMR (δ, 400 MHz, DMSO, ppm): 55.79, 114.42, 122.04, 123.38, 131.67, 132.27, 140.53, 144.20, 163.44, 167.76. Mass Spectroscopy Data: 516, 190, 165, 162, 132, 107 (Base peak) Elemental Analysis: Found (Calculated): C=60.40 (60.46); H=4.21 (4.68); N=16.25 (16.27).

N¹, N⁴-bis((1E,2E)-1-(4-chlorophenyl)-2-(hydroxyimino)ethylidene)terephthalohydrazide (L3/2C): - Yield: 74%, m. p. 214°C, UV-Visible absorption in nm (cm⁻¹): 297 (336701.03), 376 (26595.74) Infrared (KBr cm⁻¹): 3426 (O-H), 3132 (N-H), 1591 (CH=N), 1681 (C=O), 1281 (C-O), 1572 (C=C), 2981 (Csp²-H), 1010 (N-N), 952 (N-O). ¹H-NMR (δ, 400 MHz, DMSO, ppm): 7.58-7.96, multiplet, 12H (Ar-H); 8.12, s, 2H, (-CH=N); 11.01, s, 2H (NH); 13.18, s 2H (OH). ¹³C-NMR (δ, 400 MHz, DMSO, ppm): 128.75, 129.00, 129.20, 130.11, 131.61, 131.99, 138.26, 148.24, 166.93. Mass Spectroscopy Data: 524, 190, 167/169, 162, 132, 111/113 (Base Peak) Elemental Analysis: Found (Calculated): C=54.25 (54.87); H=3.29 (3.45); N=15.91 (16.00).

N¹, N⁴-bis((1E,2E)-2-(hydroxyimino)-1-(p-tolyl)ethylidene)terephthalohydrazide (L4/2D): -Yield: 78%, m. p. 154°C, UV-Visible nm(cm⁻¹): 296 (33783.76), 366 (27322.40) Infrared (KBr cm⁻¹): 3431 (O-H), 3180 (N-H), 1609 (CH=N), 1676 (C=O), 1284 (C-O), 1573 (C=C), 2976 (Csp²-H), 1017 (N-N), 952 (N-O). ¹H-NMR (δ, 400 MHz, DMSO, ppm): 7.31-7.83, multiplet, 12H (Ar-H); 7.88, s, 2H, (-CH=N); 10.70, s, 2H (NH); 12.20, s 2H (OH) & 2.37, s, 6H

(-CH₃). ¹³C-NMR (δ, 400 MHz, DMSO, ppm): 21.59, 127.83, 128.50, 129.59, 129.80, 137.93, 140.22, 143.49, 167.77. Mass Spectroscopy Data: 484, 190, 162, 147, 132, 91(Base peak). Elemental Analysis: Found (Calculated): C=64.84 (64.45); H=4.58 (4.99); N=17.22 (17.35).



Scheme 2. Synthesis of Acylhydrazoneoxime (2A, 2B, 2C & 2D)

Synthesis of complexes

The synthesis of metal complexes with zinc metal was done by using a 2:1 proportion of zinc chloride and ligands prepared by the reported²³ method respectively. The ethanolic solution of ZnCl₂ (0.04M) metal salt was mixed with the hot ligand (0.02M) ethanolic solution. The resulting reaction mixture in the flask was refluxed for three hours, then kept cool to attain room temperature before NH₃ was progressively added and constantly stirred until the mixture reached a pH range of 8.5 to 9.0. After a further sixty minutes of heating, the reaction mixture was kept to cool to attain room temperature. The separated solid material was dried in an oven at 110°C and filtered using Whatman filter paper No. 1, rinsed multiple times with hot ethanol, and dried. Over 60% of the complexes were yielded.

ZnL1: - Mol. Formula: C₂₄H₁₈Cl₂N₆O₄Zn₂,
Yield: 61%, Mol. Wt. 656.12, m. p.: 203°C; ¹H-NMR (δ, 400 MHz, DMSO, ppm): 7.35-7.99, multiplet, 14H (Ar-H); 8.28, s, 2H, (-CH=N); 10.60, s, 2H (NH). %Elemental Analysis Found (Calculated): Zn=19.86 (19.33), C=43.98 (43.93), H=2.76 (2.77), N=12.87 (12.81), Cl=10.87 (10.81), O=9.86 (9.75), Electrical conductivity: 32.027.

ZnL2: - Mol. Formula: C₂₆H₂₂Cl₂N₆O₆Zn₂,
Yield: 60%, Mol. Wt. 716.18, m. p.: 225°C; ¹H-NMR (δ, 400 MHz, DMSO, ppm): 7.12-7.92, multiplet, 12H (Ar-H), 8.10s, 2H, (-CH=N), 10.93 s, 2H (NH);

3.84s, 6H (-OCH₃). % Elemental Analysis Found (Calculated): Zn=18.31(18.26), C=43.65 (43.60), H=3.03 (3.10), N=11.73 (11.73), Cl=9.87 (9.90), O=13.49 (13.40), Electrical conductivity: 33.016.

ZnL3: - Mol. Formula: C₂₄H₁₆Cl₄N₆O₄Zn₂,
Yield: 64%, Mol. Wt. 725.01, m. p.: 232°C; ¹H-NMR (δ, 400 MHz, DMSO, ppm): 7.60-7.98m, 12H (Ar-H), 8.13s, 2H, (-CH=N), 11.03 s, 2H (NH). % Elemental Analysis Found (Calculated): Zn=18.13(18.04), C=39.71(39.76), H=2.21 (2.22), N=11.63 (11.59), Cl=19.41 (19.36), O=8.86 (8.83), Electrical conductivity: 24.018.

ZnL4: - Mol. Formula: C₂₆H₂₂Cl₂N₆O₄Zn₂,
Yield: 63%, Mol. Wt. 684.18, m. p.: 223°C; ¹H-NMR (δ, 400 MHz, DMSO, ppm): 7.33-7.86m, 12H (Ar-H), 7.89s, 2H, (-CH=N), 10.68 s, 2H (NH); 2.37s, 6H (-CH₃). % Elemental Analysis Found (Calculated): Zn=19.14 (19.11), C=45.61 (45.64), H=3.26 (3.24), N=12.25 (12.28), Cl=10.41 (10.36), O=9.39 (9.36), Electrical conductivity: 34.023.

Antimicrobial Action

The *in vitro* antibacterial screening efficacy of synthesized acylhydrazoneoxime and its metal complexes against two bacterial strains viz. *Bacillus Subtilis* as *Gram-positive* and *E. coli* as *Gram-negative* were assessed using the well diffusion method in a nutrient agar medium.

Well diffusion method

From the bacterial cultures, the microorganism's inoculums were made. Spooned into sterile, cleaned petri plates, 15 milliliters of nutrient-agar (Himedia) medium were kept to cool and solidify. Using a spreading stick, the bacterial strain broth was evenly dispersed 100 μL over the medium until it dried out. Wells of 6 mm in diameter were bored using a sterile cork borer¹². Solutions of the compounds and 100 μg/mL of streptomycin in DMSO were added to the wells, along with 100 μL of prepared bacterial strain solutions and standards. The petri plates underwent a 24-h incubation period at 37°C. As the negative control DMSO was used and streptomycin used as the positive control. The zone of inhibitions (ZI) diameters were measured to assess antibacterial activity, and each measurement was made three times.

Instrumental methods

The electrical conductivity in DMF solvent was measured using an Equiptronics conductivity

meter (EQ-664A). UV-Visible spectral data in the 200–900 nm region were collected on the Jasco V770 UV-Vis spectrophotometer using DMF as a solvent. Using a Rigaku Thermo Plus-8120 TG-DTA apparatus by using a nitrogen environment and heating rate of $10^{\circ}\text{C min}^{-1}$, metal complex TG-DTA analysis was carried out, with alumina serving as a reference. KBr pallets were used to collect the infrared spectra of complexes on a Perkin-Elmer analyzer in the $4000\text{--}400\text{ cm}^{-1}$ range. At room temperature, the magnetic susceptibility data of every zinc complex prepared was determined using Gouy's method.

RESULTS AND DISCUSSIONS

All of the complexes exhibited a yellowish color, were soluble in DMSO and DMF but insoluble in water and the majority of other typical organic solvents. They were also stable at room temperature. For every metal complex, the metal:ligand stoichiometry is 2:1.

UV-Visible Spectra

For ligands

The acylhydrazoneoxime ligands undergo electromagnetic radiation absorption in UV-Visible regions involving electronic excitations of σ , π , or non-bonding electrons from lower energy level bonding molecular orbital level to higher energy anti-bonding or non-bonding orbital. There were two types of transitions $n\rightarrow\sigma^*$ and $\sigma\rightarrow\sigma^*$. An auxochrome having unshared electrons when in conjugation with a chromophore can cause changes in both

wavelength (λ_{max}) as well as intensity. If auxochrome-like hydroxyl (-OH) is present in the molecule it also shows $n\rightarrow\sigma^*$ transition which is also called the auxochromic effect.

The visible and UV spectrums of synthesized hydrazone ligands were observed in a Jasco V770 UV-Visible spectrophotometer in the region of 200–800 nm ($50000\text{--}12500\text{ cm}^{-1}$). All hydrazone ligands show the $\pi\rightarrow\pi^*$ and $n\rightarrow\pi^*$ transitions exhibit bands in their electronic spectra between 296 and 381 nm ($33783.76\text{--}26246.72\text{ cm}^{-1}$).

For complexes

Using a Jasco V770 UV-Visible spectrophotometer in the 200–800 nm range in DMF, the UV-Visible spectral bands of the synthesized zinc complexes were obtained. The important band observed for acylhydrazoneoxime zinc complexes is summarized in Table 1. The electronic spectra show a band between 288 nm (34722 cm^{-1}) - 290 nm (34483 cm^{-1}) which is due to the intra-ligand transition $\pi\rightarrow\pi^*$ and another band at 343 nm (29155 cm^{-1})–353 nm (28329 cm^{-1}) for $n\rightarrow\pi^*$. The absorption band between 382 nm (26178 cm^{-1}) – 396 nm (25553 cm^{-1}) is due to charge transfer transition (CT). The absence of d-d transitions in the visible range indicates the absence of unpaired electrons. The present Zn^{2+} complexes have tetrahedral geometry which is also in excellent agreement with the data on magnetic susceptibility. Fig. 1 demonstrates the UV-Visible spectra of zinc complexes.

Table 1: Electronic spectrum data, $\lambda(\text{nm})$ and $\nu(\text{cm}^{-1})$ for zinc metal complexes

ZnL_1		ZnL_2		ZnL_3		ZnL_4		Assignment
$\lambda(\text{nm})$	$\nu(\text{cm}^{-1})$	$\lambda(\text{nm})$	$\nu(\text{cm}^{-1})$	$\lambda(\text{nm})$	$\nu(\text{cm}^{-1})$	$\lambda(\text{nm})$	$\nu(\text{cm}^{-1})$	
392	25510	396	25553	390	25641	382	26178	Charge Transfer Transition
348	28736	353	28329	343	29155	351	28490	Intra ligand transition
290	34483	288	34722	290	34483	288	34722	Intra ligand transition

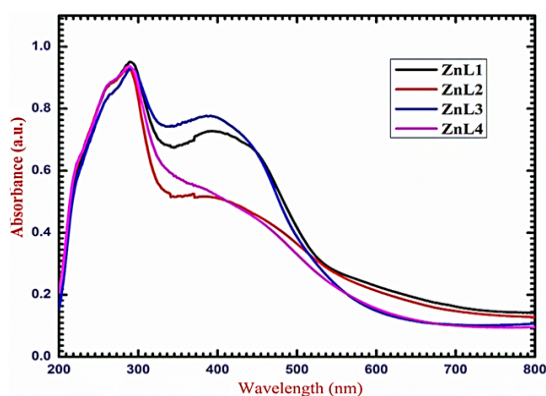


Fig. 1. UV-Visible spectra of Zinc Metal Complexes

Infrared Spectra

For ligands

Lambda 7600 PC FT-IR spectrophotometer (range $400\text{--}4000\text{ cm}^{-1}$). The infrared absorption bands along with the ligand assignments for acylhydrazoneoxime were shown here. The identified bands are attributed to (C=N) oxime, (C=H) amide, (C=N) imine, (O-H), (C-N), (N-O), and (C-N). The distinctive amide (C=O) band may be seen at $1676\text{--}1720\text{ cm}^{-1}$ in the FTIR spectral data of the acylhydrazoneoxime ligands. At $1609\text{--}1635\text{ cm}^{-1}$ and $1560\text{--}1571\text{ cm}^{-1}$, respectively, the stretching vibrations of the (C=N) imine and (C=N) oxime

were seen. The distinctive (O-H) oxime absorption is attributed to the broad medium-intensity band that appears between 3413 and 3440 cm^{-1} . These results agree with the hydrazone and oxime derivatives that have been previously reported^{20,25,27}.

The infrared spectra of acylhydrazoneoxime show a very broad low-intensity peak situated between 3300 and 2600 cm^{-1} . This region is associated with the intramolecular H-bonding vibration ($\text{O-H}\cdots\text{N}$) in regions^{20,25,27}. In addition, the amide $\nu(\text{N-H})$ stretching band 3132-3193 cm^{-1} of the ligands was not visible in the infrared spectra, most likely because it overlapped with the intermolecular hydrogen-bonded O-H stretching frequency.

For complexes

Table 2 shows the infrared spectral bands of the zinc metal complexes acylhydrazoneoxime and their corresponding assignments. The bands observed that are attributed to $\nu_{(\text{C}=\text{N})}$ oxime, $\nu_{(\text{C}=\text{O})}$ amide, $\nu_{(\text{C}=\text{N})}$ imine, $\nu_{(\text{O-H})}$, $\nu_{(\text{N-H})}$, $\nu_{(\text{C-N})}$, $\nu_{(\text{N-N})}$ and also for $\nu_{(\text{Zn-O})}$ and $\nu_{(\text{Zn-N})}$. Acylhydrazoneoxime zinc metal complexes exhibit the distinctive amide $\nu(\text{C}=\text{O})$ band

coordinated in their infrared spectra with Zn metal appearing at 1628-1595 cm^{-1} which is lower than ligand frequency indicates coordination of oxygen to zinc metal and is also supported by The new band for $\text{O}\rightarrow\text{Zn}$ appears between 490 and 468 cm^{-1} . At 1550–1528 cm^{-1} and 1517–1481, respectively, the stretching vibrational frequency of the $\nu(\text{C}=\text{N})$ oxime and $\nu(\text{C}=\text{N})$ imine were seen, both are coordinated with Zn metal so their frequencies are lower than ligand frequencies, and further supported by the appearance of new bands for Zn-N (646-624 cm^{-1}) and $\text{N}\rightarrow\text{Zn}$ (535-501 cm^{-1}). The broad band of medium intensity that is visible in ligand spectra at around 3547-3502 cm^{-1} is recognized as the characteristic $\nu(\text{O-H})$ oxime disappeared in complexes indicating deprotonation and supported by the appearance of peak for N O (1026-1003 cm^{-1}). These values correspond with the previously reported²⁸⁻²⁹ acylhydrazoneoxime zinc metal complexes. The infrared spectra of zinc metal complexes did not clearly show the amide $\nu(\text{N-H})$ stretching band 3324-3301 cm^{-1} , most likely because it overlapped with the intermolecular hydrogen bonded $\nu(\text{O-H})$ stretching vibrational frequency. Fig. 2 demonstrates the infrared spectra of zinc complexes.

Table 2: FTIR bands (cm^{-1}) for the zinc complexes

Complex	$\nu(\text{N-H})$	$\nu(\text{C}=\text{O})$	$\nu(\text{C}=\text{N})$ imine	$\nu(\text{C}=\text{N})$ oxime	$\nu(\text{C-N})$	$\nu(\text{N O})$	$\nu(\text{N-N})$	$\nu(\text{Zn-N})$	$\nu(\text{N Zn})$	$\nu(\text{O Zn})$
ZnL ₁	3324	1628	1550	1461	1405	1015	1093	646	501	490
ZnL ₂	3313	1595	1539	1483	1405	1026	1104	635	535	479
ZnL ₃	3307	1606	1539	1517	1394	1003	1082	646	535	468
ZnL ₃	3312	1595	1528	1494	1427	1012	1083	624	501	490

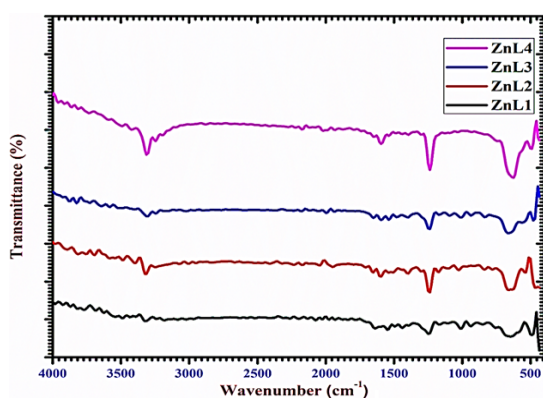


Fig. 2. Infrared Spectra of Zinc Metal Complexes

¹H-NMR Spectra

The synthesized acylhydrazoneoxime's ¹H-NMR spectra indicate that, in an imine environment, the N-H proton resonance appears as a singlet at 10.59–11.01 ppm. At 12.20–13.18 ppm, the distinctive oxime O-H proton is seen as a

singlet, confirming the existence of intramolecular hydrogen bonding. These shifts in chemical composition are characteristic⁴ values for oximes and hydrazones. The characteristic shift appears as a singlet at 3.85 ppm for substituted ($-\text{OCH}_3$) for 2B and 2.37 ppm for substituted ($-\text{CH}_3$) for 2D. The additional measurements for the hydrazone compound's ¹H-NMR chemical shifts were Ar-H at 7.01–7.96 ppm and CH at 7.88–8.29 ppm. These results match up with the previously published^{4,25} relevant substances. Fig. 3 demonstrates the NMR spectra of Ligand L1.

¹³C-NMR Spectra

The typical imine peak which appears in the region 138 to 149 ppm is predicted for C=N moiety. ¹³C Spectra also shows peaks in the region of 127-136 ppm corresponding to aromatic carbons. The characteristic peak of aromatic amide carbon

(C=O) atoms appears between 166 to 189 ppm in the ^{13}C spectra of ligands.

Mass Spectroscopy Data

The Mass spectral data show intense molecular ion peaks, they also show characteristic dihydrazide, amide fragments, and one fragment between hydrazones C=O group and support the completion of the reaction.

Electrical Conductance

The molar conductance values observed for all zinc metal complexes fall between 24.018 to 34.023 $\text{mhos.cm}^2\text{mol}^{-1}$ in DMSO in a concentration of 10^{-3} M are high suggesting that the complexes are electrolytic in nature.

Measurement of Magnetic Susceptibility

Using $\text{Hg}[\text{Co}(\text{SCN})_4]$ as a calibrant, the magnetic susceptibility of each zinc complex was observed at room temperature using Gouy's method. Based on their magnetic moments, all of the complexes (ZnL1, ZnL2, ZnL3, and ZnL4) show diamagnetic behavior at room temperature.

Thermal Analysis

The current complexes were subjected to a $10^\circ\text{C}/\text{min}$ heating rate in an inert nitrogen environment for the TG-DTA analysis. The thermographs shown in Fig. 4 (a to d) are indicating continuous mass loss of ligand part with increasing temperature. The metal complexes are thermally stable and decompose above 200°C and give zinc oxide as the ultimate product²¹ of heating above 600°C as reported. Fig. 5a reveals the proposed bonding structure of the complexes and Fig. 5b reveals the 3D bonding structure of the ZnL1 complex.

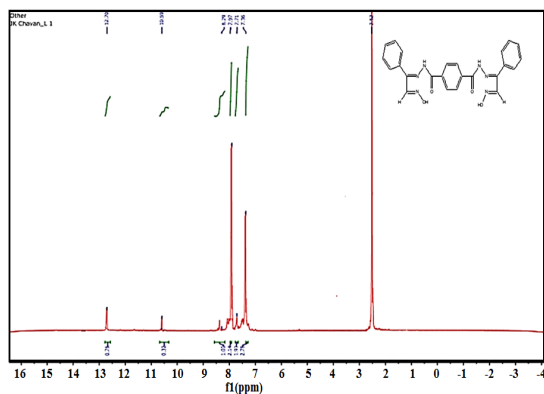


Fig. 3. Ligand NMR for Ligand L1

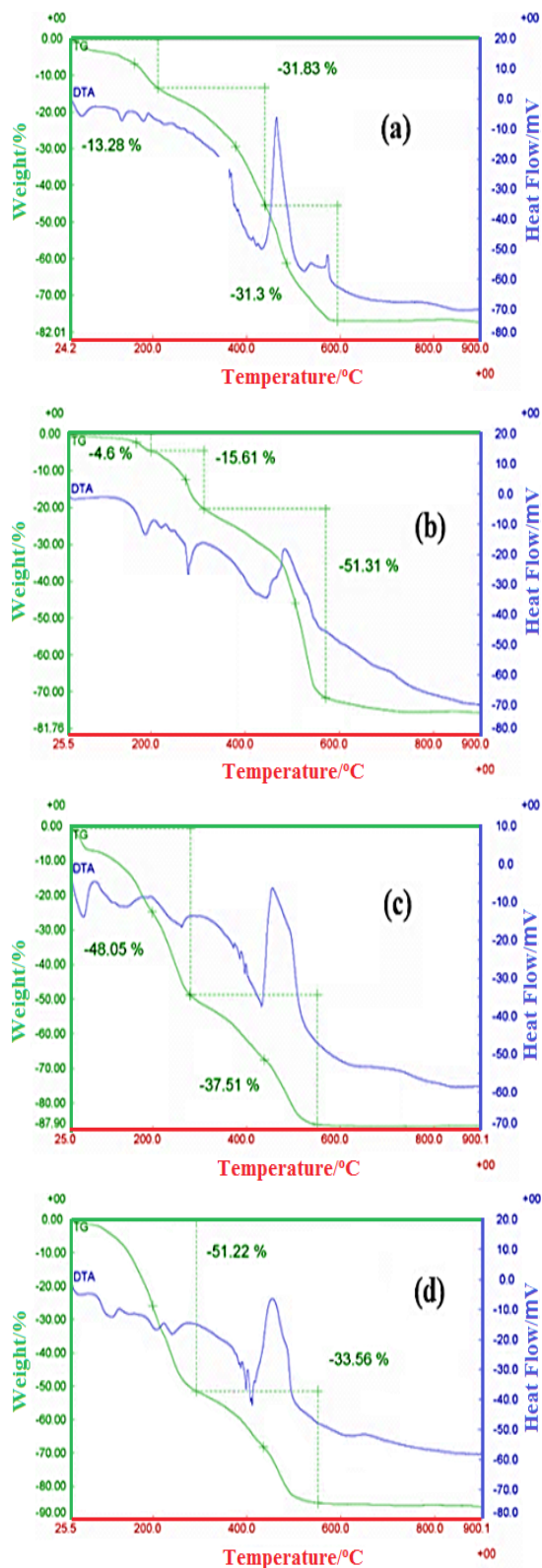
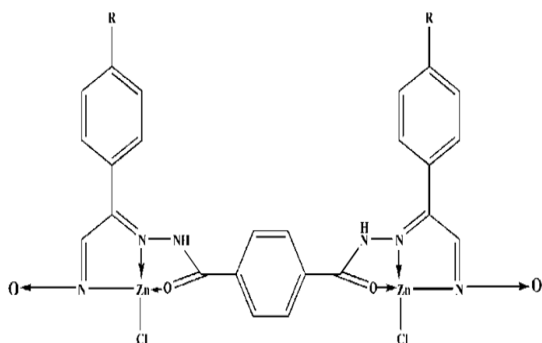


Fig. 4. TG-DTA of (a) ZnL1, (b) ZnL2, (c) ZnL3 and (d) ZnL4



15

Fig. 5(a). The Proposed bonding structure of the complexes ZnL_1 (R=H), ZnL_2 (R=OCH₃), ZnL_3 (R=Cl) and ZnL_4 (R=CH₃)

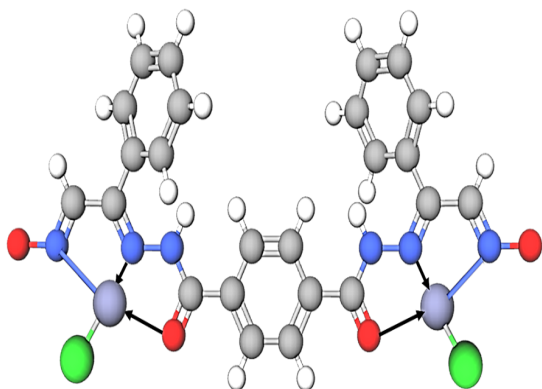


Fig. 5(b). The Proposed bonding 3D structure of the ligand ZnL_1 ,
Study of antimicrobial activities of acylhydrazone oxime zinc metal complexes

The findings of the *in vitro* antimicrobial screening are displayed in Table 3. ZnL_1 , ZnL_2 , ZnL_3 , ZnL_4 , and a reference chemical streptomycin were tested for their antibacterial activity by measuring the zone of inhibition using the well diffusion method against *Gram-positive* and *Gram-negative Bacillus Subtillis* (ATCC 6633) and *Escherichia coli* (NCIM 2832) bacterial strains. The present zinc complexes exhibited good antibacterial activity shown in Fig. 6(a) and 6(b). The antimicrobial activity of all the acylhydrazoneoxime zinc metal complexes is less than that of standard streptomycin.

Table 3: Antimicrobial activity of the complexes

Sr. No	Samples	Zone in diameter (mm)	
		<i>Bacillus subtilis</i>	<i>E. coli</i>
1	Control	0	0
2	Standard (Streptomycin)	24	24
3	ZnL_1	20	06
4	ZnL_2	14	08
5	ZnL_3	08	09
6	ZnL_4	12	08

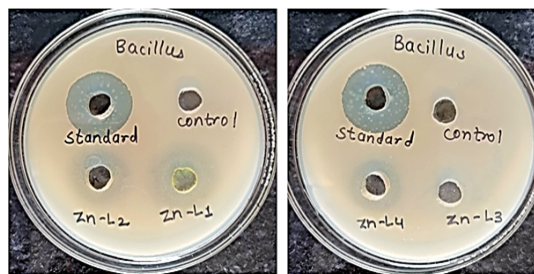


Fig. 6(a). Antibacterial activity of *Bacillus subtilis*

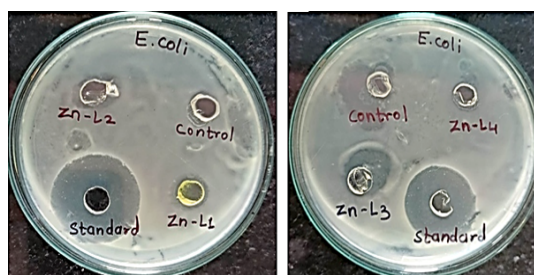


Fig. 6(b). Antibacterial activity of *E. coli*

CONCLUSION

The complexes exhibit strong metal-ligand bonding and an electrolytic character, as indicated by their higher decomposition temperature and electrical conductivity tests, respectively. The electronic spectral data confirm that the Zn(II) complexes have a tetrahedral geometry and are diamagnetic, as suggested by room temperature magnetic investigations. The bonding of the metal through the ligands' N and O donor atoms is seen in the IR spectra.

ACKNOWLEDGEMENT

The authors would like to express gratitude to SAIF, Shivaji University, Kolhapur, The Institute of Science, Mumbai; Infinite Biotech; Institute of Research and Analytics, Sangali; and Shri Yashwantrao Patil Science College, Solankur, for supplying the required equipment.

Conflict of Interest

The authors declare that there is no conflict of interest.

REFERENCES

1. Iskander M. F.; Sayed L.; El Salem N. M. H.; Werner R. and Haase W., *J. Coord. Chem.*, **2003**, *56*(12), 1075-1084.
2. Bat H. and Dege N., *Journal of Molecular Structure.*, **2018**, *1162*, 125-139.
3. El-tabl A. S.; El-waheed M. M. A. and Shakdofa M. M. E., *Main Group Chemistry.*, **2013**, *12*, 153-168.
4. Gup R. and Giziroglu E., *Spectrochimica Acta Part-A.*, **2006**, *65*, 719-726.
5. Tarve S. S.; Prabhulkar S. G. and Patil R. M., *Indian Journal of Research.*, **2016**, *5*(8), 195-199.
6. Tarve S. S.; Prabhulkar S. G. and Patil R. M., *Indian Journal of Research.*, **2016**, *5*(9), 259-263.
7. Abraham F.; Capon J. M.; Nowogrocki G.; Sueur S. and Bremard C., *Polyhedron.*, **1985**, *4*(10), 1761-1767.
8. Kaminsky W., Jasinski J. P., Woudenberg R., Goldberg K. I. and West, D. X., *Journal of Molecular Structure.*, **2002**, *608*, 0-6.
9. Maekawa M.; Kitagawa S.; Nakao Y. and Sakamoto S., *Inorganica Chimica Acta.*, **1999**, *293*, 20-29.
10. Wan S. P.; Mori W. and Yamada S., *Synthesis and Reactivity in Inorganic and Metal-Organic Chemistry.*, **1986**, *16*(9), 1273-1288.
11. Giziroglu E.; Sarikurkcü C. and Sarac N., *Journal of Applied Pharmaceutical Science.*, **2015**, *5*, 48-55.
12. Junghare N. V.; Jagtap S. B.; Jadhav R. R. and Jadhav J. P., *Oriental Journal of Chemistry.*, **2022**, *38*(2), 238-246.
13. Lad M. N.; Patil R. M. and Sathe G. B., *Research Journal of Chemistry and Environment.*, **2020**, *24*(6), 122-124.
14. Lad M. N., Patil R. M. and Yamgar B. A., *Research Journal of Chemistry and Environment.*, **2022**, *26*(1), 104-109.
15. Patil R.M., *Drug Synthesis.*, **2007**, *64*(4), 345-353.
16. Al-Ne'aimi M. M.; Al-Khuder M. M. and Mohammed S. J., *J. Sci.*, **2012**, *23*(4), 51-69.
17. Mandal H.; Chakrabartty S. and Ray D., *RSC Adv.*, **2014**, *4*, 65044-65055.
18. Koh L. L.; Kon O.L.; Loh K.W.; Long Y. C., Ranford J. D., Tan A.L.C. and Tjan Y. Y., *Journal of Inorganic Biochemistry.*, **1998**, *72*, 155-162.
19. Zhao Xiao-Jun.; Xue Ling-Wei & Zhang Cai-Xia., *Synthesis and Reactivity in Inorganic, Metal-Organic, and Nano-Metal Chemistry.*, **2015**, *45*, 516-520.
20. Al-Ne'aimi M.M.; Al-Khuder M.M., *Spectrochimica Acta Part A: Molecular and Biomolecular Spectroscopy.*, **2013**, *105*, 365-373.
21. Mostafa M. M., Khattab M. A. and Ibrahim K. M., *Polyhedron.*, **1983**, *2*(7), 583-585.
22. El-Tabl A S.; Farag A., *Journal of Coordination Chemistry.*, **2010**, *63*(4), 700-712.
23. Chavan J. K. and Patil R. M., *Research Journal of Chemistry and Environment.*, **2023**, *27*(12), 31-34.
24. El-Saied F., Salem T. A., Shakdofa M. M. E., Al-Hakimi A. N., Ahmed S., Beni-Suef University *Journal of Basic and Applied Sciences.*, **2018**, *7*, 420-429.
25. Gup R. and Kirkan B., *Spectrochimica Acta Part-A.*, **2005**, *62*, 1188-1195.
26. Zhang S.-H.; Feng C., *Journal of Molecular Structure.*, **2010**, *977*, 62-66.
27. Bagrov F.V and Vasil T. V., *Russian Journal of Organic Chemistry.*, **2002**, *38*(9), 1309-1313.
28. Sulaiman M.M.; Mohammed S.J., *International Journal of Science and Research.*, **2017**, *6*(11), 535-547.
29. Szecsenyi K. M.; Leovac V.M.; Jaaeimovieae Z. K.; Ee.ljeviae V. I.; Kovacs A.; Pokol G. and Gal S., *Journal of Thermal Analysis and Calorimetry.*, **2001**, *63*, 723-732.